



RESEARCH ARTICLE

The Life Cycle and Net Radiative Effect of Tropical Anvil Clouds

10.1029/2018MS001484

Key Points:

- The life cycle of extended anvil clouds can yield a near neutral cloud radiative effect
- Anvil lifetimes are increased by radiatively driven turbulence within the cloud
- Vapor can be recycled by radiative, microphysical, and turbulent interactions in anvil clouds

Correspondence to:

D. L. Hartmann,  
dhartm@uw.edu

Citation:

Hartmann, D. L., Gasparini, B., Berry, S. E., & Blossey, P. N. (2018). The life cycle and net radiative effect of tropical anvil clouds. *Journal of Advances in Modeling Earth Systems*, 10. <https://doi.org/10.1029/2018MS001484>

Received 24 AUG 2018

Accepted 18 NOV 2018

Accepted article online 22 NOV 2018

Dennis L. Hartmann<sup>1</sup> , Blaž Gasparini<sup>1</sup>, Sara E. Berry<sup>2</sup> , and Peter N. Blossey<sup>1</sup>

<sup>1</sup>Department of Atmospheric Sciences, University of Washington, Seattle, WA, USA, <sup>2</sup>Epic Systems, Verona, WI, USA

**Abstract** We explore the importance of the life cycle of detrained tropical anvil clouds in producing a weak net cloud radiative effect (NCRE) by tropical convective systems. We simulate a horizontally homogeneous elevated ice cloud in a 2-D framework using the System for Atmospheric Modeling cloud-resolving model. The initially thick cloud produces a negative NCRE, which is later canceled by a positive NCRE as the cloud thins and rises. Turning off interactive cloud radiation reveals that cloud radiative heating and in-cloud convection are fundamental in driving net radiative neutrality. In-cloud convection acts to thin initially thick anvil clouds and loft and maintain thin cirrus. The maintenance of anvil clouds is tied to the recycling of water vapor and cloud ice through sublimation, nucleation, and deposition as air parcels circulate vertically within the cloud layer. Without interactive radiation, the cloud sediments and sublimates away, producing a large negative NCRE. The specification of cloud microphysics substantially influences the cloud's behavior and life cycle, but the tendency of the life cycle to produce compensating cloud radiative effects is robust to substantial changes in the microphysics. Our study shows that small-scale processes within upper level ice clouds likely have a strong influence on the NCRE associated with tropical convective cloud systems.

**Plain Language Summary** Clouds can either warm or cool the Earth, depending on the ratio between the solar radiation they reflect and the amount by which they reduce the emission of radiation to space. In the warm regions of the tropical oceans, these solar and terrestrial radiation effects cancel nearly exactly, so that tropical convective clouds do not appear to change the Earth's energy balance as measured from space. Neither the reason why this close balance occurs nor whether this balance will change as the Earth warms or cools is understood. In this paper we use a high-resolution model to show that the layer of ice delivered to the atmosphere by tropical convection goes through a life cycle from thick to thin and that this life cycle tends to produce a balanced net radiative effect of the cloud, as observed. To resolve the key processes in a climate model will require simulation or parameterization of interactions among radiative heating of the ice cloud, small-scale convection within the ice cloud, and cloud physical processes that tend to shape the net radiative effect of the cloud through its lifetime.

1. Introduction

Clouds have a significant impact on the radiation budget of the Earth for both longwave (LW) and short-wave (SW) radiation. Tropical convective clouds include convective cores, rainy anvils, and thinning anvil clouds. The cloud morphology of specific regions can have large impacts not only on the local climate but also on larger-scale processes. These clouds have the ability to alter the environmental temperature profile (Liou, 1986), large-scale vertical motions (Houze, 1982), and upward mass transport (Ackerman et al., 1988; Sherwood, 1999). Thick convective clouds in the tropics can have a net cooling effect, since their effect on reflected SW is larger than their effect on emitted LW. As these clouds spread and become thinner, their SW cloud radiative effect (SWCRE) becomes smaller, while the LW cloud radiative effect (LWCRE) remains large, giving a positive net cloud radiative effect (NCRE) in the latter stages of their life cycle. The relationship of tropical anvil cloud volume to the mesoscale convective systems that feed them has been studied observationally by Deng et al. (2016). In this paper we will use the term extended anvil cloud to denote the portion of *cumulonimbus incus* that extends away from convection and has a layer of clear air below it. In the tropics these extended anvils center around 200 hPa, since most of the ice detrains well below the tropical tropopause.

Despite having a large SWCRE and LWCRE at the top of the atmosphere, the NCRE of convective systems over the warm tropics is known to be small so that the net radiation in convective and adjacent clear areas is about the same (Harrison et al., 1990; Hartmann & Short, 1980; Hartmann et al., 1992, 2001; Ramanathan et al., 1989).

©2018. The Authors.  
This is an open access article under the terms of the Creative Commons Attribution-NonCommercial-NoDerivs License, which permits use and distribution in any medium, provided the original work is properly cited, the use is non-commercial and no modifications or adaptations are made.

That is to say, the overall NCRE of these cloud systems is neutral. As shown in Hartmann and Berry (2017), Hartmann et al. (2001), and Berry and Mace (2014), a diverse distribution of cloud types acts to maintain the observed radiative neutrality at the top of the atmosphere (TOA). Tropical convective clouds have a wide range of outgoing LW radiation (OLR) and albedo values, depending on the vertical distribution of cloud water and ice content, so that these clouds have a wide range of individual net radiative effects. The aggregate effect is neutral, but if this aggregate effect changes in a warmed climate, a significant feedback could be produced. For this reason it is important to understand the causes of the neutral effect of tropical deep convective cloud and whether the processes that produce it are being simulated correctly in climate models.

In order to accurately assess the larger-scale impacts of anvil clouds, we need to understand what controls the distribution of their albedo and OLR, which is related to their macrophysical and microphysical properties. The atmospheric radiative heating associated with anvils is significant in the middle and upper troposphere, and overall is more important than the radiative effects of the connected convective towers (Ackerman et al., 1988; Mapes & Houze, 1993). Sufficiently thick anvil clouds are heated at the bottom by LW heating from the below and cooled at the top by LW emission from the cloud. Thus, radiation drives instability in elevated ice clouds, which can drive in-cloud convection (Churchill & Houze, 1991). Fu et al. (1995) and Harrop and Hartmann (2016) found that the effect of radiation on clouds extended the lifetime and areal extent of elevated ice cloud layers. Convection and radiation continue to play an important role even as anvil clouds thin to subvisible cirrus (Gu & Liou, 2000).

Small ice particles sediment slowly and can have substantial microphysical and radiative effects (Zender & Kiehl, 1994). The specification of ice particle sedimentation rate in global climate models can have a strong effect of their estimates of climate sensitivity (Sanderson et al., 2008). The abundance and properties of ice clouds in climate models is very sensitive to assumptions about the concentration of small (radius < 30  $\mu\text{m}$ ) ice particles (Mitchell et al., 2008). Measurements of ice particle concentrations are limited to particles larger than about 10  $\mu\text{m}$  and are subject to biases associated with shattering of larger particles (Jensen et al., 2009; Korolev et al., 2013). Modeling suggests that particle concentrations formed by nucleation are very sensitive to vertical velocities produced by waves or turbulence (Jensen, Ueyama, Pfister, Bui, Alexander, et al., 2016), and that in such cases nucleation is not too sensitive to the presence of ice nuclei (Jensen, Ueyama, Pfister, Bui, Lawson, et al., 2016), although the relative importance of homogeneous and heterogeneous nucleation is a subject of continuing research. Here we will investigate the effects of the positive feedback between ice nucleation and the turbulence generated by the atmospheric radiative effect of ice clouds.

Thin cirrus clouds have been studied extensively with cloud-resolving models. Dinh et al. (2010) found that mesoscale circulations associated with isolated cirrus clouds near the tropopause transition layer are fundamentally important for cloud maintenance. Thermally forced circulations feed water vapor from the surrounding environment into the cloud, leading to water vapor convergence and particle growth. Jensen et al. (2011) also noted the role of heating in extending the lifetimes of tropopause transition layer cirrus. The convergence opposes sublimation and sedimentation of cloud ice. Contrarily, Boehm et al. (1999) found that thin cirrus clouds could not sustain themselves long enough against sedimentation and evaporation to form such circulations, instead hypothesizing that some large-scale upward motion is required. Dobbie and Jonas (2001) studied the role of radiation in driving thick ice clouds using a two-dimensional eddy-resolving model and found that radiative heating drove convection in the layer, which increased the persistence of the cloud. Other studies have investigated thicker ice cloud varieties by representing deep convective systems in cloud-resolving models, such as System for Atmospheric Modeling (SAM) and the Weather Research and Forecasting Model (WRF), under various atmospheric conditions and model frameworks by first initiating the deep convection, then tracking it through its life cycle (Chen et al., 1997; Fan et al., 2010; Fu et al., 1995). Radiative convective simulations with simple bulk microphysical schemes do not simulate the observed distribution of OLR and albedo, although the microphysics can be tuned to do so (Lopez et al., 2009). Powell et al. (2012) tested a wide variety of microphysics schemes for their ability to match remote sensing data of tropical continental anvil clouds. They found a wide variety of behaviors for different microphysics schemes, with simpler schemes matching the data better than more complex ones.

Hartmann and Berry (2017) used Clouds and the Earth's Radiant Energy System (CERES) and CloudSat/Calipso data to show that the neutrality of tropical convective clouds results from cancellation between the negative NCRE of deep, rainy core clouds and the positive effect of thinning ice clouds and concluded that both types of

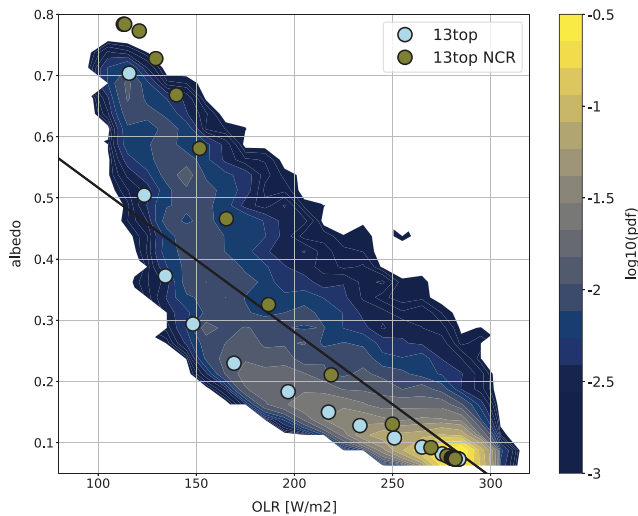


**Figure 1.** Probability density of OLR and albedo from Clouds and the Earth's Radiant Energy System pixel measurements from the Tropical West Pacific (12S to 12N, 150E to 170E) during July and August as in Hartmann and Berry (2017). Superimposed are the trajectories of OLR and albedo for numerical experiments conducted here for an initial ice cloud extending from 8.2 to 13 km. Each dot represents a time separated by 1.5 hr. The initial conditions for the control and NCR interactions cases overlap exactly. The black line indicates albedo-OLR pairings for which the cloud is radiatively neutral. NCR = no cloud radiation; OLR = outgoing longwave radiation.

clouds were produced in individual tropical convective cloud systems. Wall et al. (2018) followed the life cycles of convective complexes using geosynchronous data and showed the evolution of radiative properties. Wall and Hartmann (2018) showed that the response of NCRE to upward motion is weak because the proportion of thin and thick anvils remains almost constant as the large-scale vertical velocity increases and that climate models may not have this quality if they lack sufficient thin anvil cloud. Motivated by this work, we hypothesize that the life cycle of anvil clouds in a deep convective system is a key contributor to the TOA radiative neutrality of convective clouds in the tropics. The natural life cycle involves an initially thick rainy anvil region, which might have a negative radiative effect, but it evolves into a larger area of thin elevated cloud, which could have a compensating positive radiative effect. We anticipate that radiative, convective, and microphysical processes within the anvil cloud are important in determining the properties and fractional abundance of the thinning anvil cloud. We test this hypothesis in a simple modeling framework, in which the anvil cloud is two-dimensional and periodic in the horizontal dimension.

The model is initialized with horizontally uniform upper level ice clouds with varying thickness. In this framework we are able to study the role of radiatively driven turbulence in modifying the upper level ice cloud distinct from a time-varying supply of ice from active deep convection and spreading of anvil clouds by radiatively driven circulations as in Dinh et al. (2010). We find that radiatively driven turbulence within the elevated ice cloud supports a mechanism whereby ice is recycled from ice to vapor to ice again within the cloud, which leads to greater persistence of the thinning elevated ice cloud.

As motivation for this study we show in Figure 1 the observed probability density function (pdf) of OLR-albedo pairings in the tropical west Pacific for the nadir pixel from the CERES data set (Wielicki et al., 1996) as described in Hartmann and Berry (2017). Superimposed on this pdf are the OLR and albedo pairings every 1.5 hr during our anvil life cycle simulation for an ice cloud that at initiation has a top at 13 km and a base at 8.2 km. A top at 13 km gives a cloud top temperature closer to 215 K consistent with the Fixed Anvil Temperature (FAT) hypothesis (Hartmann & Larson, 2002). Figure 1a shows that the history of our simulated anvil traces out a curve in OLR-albedo space that is similar to the observed pdf, with the initial state of the simulation indicating the cold topped, high-albedo cloud. The latter stages of the life cycle are represented by the circles at lower albedo and higher OLR values, with the closer spacing of the circles indicating that the model persists longer in these states, which is consistent with the much more frequent occurrence of these thin ice clouds in observations. The simple model experiments here thus predict the high frequency of relatively high-OLR, low-albedo clouds that are in fact high, thin ice clouds (Hartmann & Berry, 2017). A case in which the radiative effect of the clouds is not felt by the simulation (NCR case) is also shown. In this case the simulation stays too long in the high-albedo low-OLR regime and also does not simulate the long residence time in the thin cirrus regime with low albedo and high OLR.

We use three microphysics parameterizations to test the sensitivity of the results to the particular microphysics chosen. Three-dimensional simulations with a uniform cloud across the domain produce nearly identical results to the two-dimensional simulations shown here. An initial condition in which the ice cloud occupies only part of a three-dimensional domain also shows that radiation is critical for the evolution of the albedo-OLR distribution. Any process that adds moisture to the upper troposphere, such as additional deep convection or large-scale ascent, will compete with the stratiform cloud processes featured here and reduce their relative importance. We leave it to later work involving more intensive computations to determine whether the mechanisms we highlight here can compete with the neglected processes.

The model framework is described in section 2. Results from our model simulations are shown in section 3, followed by a discussion of implications, model sensitivities, and caveats in section 4. A summary and discussion are provided in section 5.

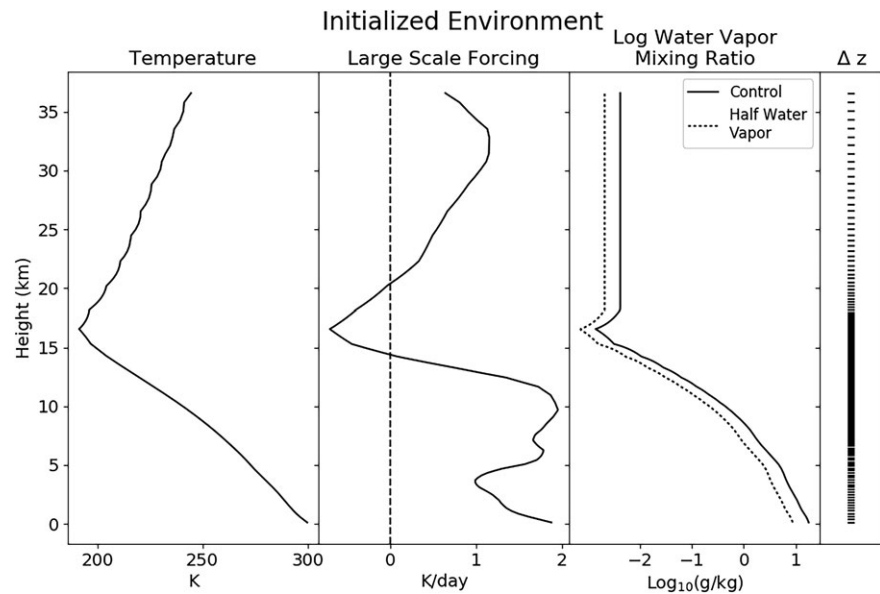


**Figure 2.** Background profiles used to initialize the model. From left to right: mean temperature sounding profile from Tropical Ocean Global Atmosphere Coupled Ocean-Atmosphere Response Experiment, applied large-scale forcing to counteract clear-sky radiative cooling, mean water vapor profile from Tropical Ocean Global Atmosphere Coupled Ocean-Atmosphere Response Experiment and halved profile used in the sensitivity test *half water vapor* (see Table 1), and model vertical resolution.

## 2. Methods

### 2.1. Model Details

We use the SAM cloud-resolving model version 6.10.6 (Khairoutdinov & Randall, 2003) in a 2-D framework. Simulations are run with a horizontal periodic boundary condition and a fixed sea surface temperature of 302.1 K. The effects of subgrid-scale motions are handled with a 1.5-order closure scheme that incorporates a simple Smagorinsky-type scheme. Model radiation is calculated using the rapid and accurate radiative transfer model for GCMs (Mlawer et al., 1997), which is called every six time steps (i.e., every 30 s with our 5-s time step). Both ice and snow are radiatively active. Morrison et al. (2005) double-moment microphysics scheme (M2005) is used for most of the simulations shown. The sensitivity of our results to this choice is tested by also doing experiments with the Thompson et al. (2007) microphysics scheme and the predicted particle properties (P3) scheme (Morrison & Milbrandt, 2015). The radiative size of snow and cloud ice in the Thompson microphysics are computed following Fu (1996). The projected area of snow is computed by integrating the parameterization of snow crystal *area ratio* in Heymsfield & Miloshevich (2003; equation (2)) across the snow size distribution using the parameterization of Field et al. (2005). The radiative properties of snow and cloud ice in M2005 are taken from the lookup tables generated for the Community Atmosphere Model, version 5, as described in Gettelman et al. (2010, section 2.5). Cloud ice particles are initialized with a radius of 40  $\mu\text{m}$ . Neither rotation nor diurnal cycle are present in these simulations. The solar zenith angle is fixed to the insolation-weighted daily average value of  $42.89^\circ$  and the solar constant is adjusted to  $578.0 \text{ W/m}^2$  to give an equivalent insolation of  $423.5 \text{ W/m}^2$ , which is near the tropical average. No mean winds are present at the start of the simulations.

The total horizontal domain size is 32 km with 250-m grid spacing unless otherwise noted. The vertical grid is displayed in Figure 2 and includes 320 model levels. The highest vertical resolution of 25 m occurs between 12 and 16 km above ground level. The important results are not sensitive to factors of 2 change of spatial resolution. Strong Newtonian damping is applied in the upper third of the model domain. We initialize the model sounding with the average temperature and water vapor profiles from the Tropical Ocean Global Atmosphere Coupled Ocean-Atmosphere Response Experiment. A large-scale temperature forcing is applied to balance the clear-sky radiative cooling associated with the initial temperature and humidity fields, as shown in Figure 2. The large-scale temperature forcing stands in for the large-scale subsidence that in nature would balance the clear-sky radiative cooling. Removing this large-scale temperature forcing has very little effect on

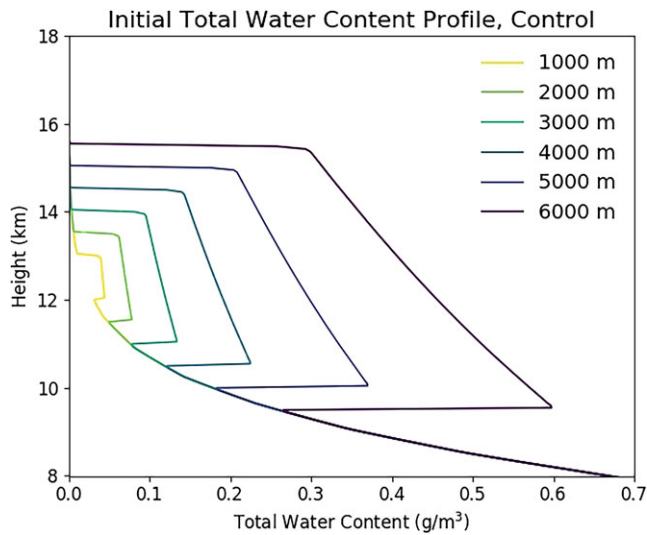


**Figure 3.** Vertical profiles of initialized total water content (water vapor + cloud ice) for the six initial cloud depths in the control case. Profiles are constructed such that the clouds have vertically uniform total water mixing ratio and liquid ice static energy.

the simulations, because the radiative heating rates associated with the presence of the ice cloud exceed the temperature forcing by more than an order of magnitude.

## 2.2. Cloud Initialization

Since anvil clouds are very large in extent, often covering  $10^5$  km<sup>2</sup> (Mapes & Houze, 1993; Protopapadaki et al., 2017), we initialize our simulations with a horizontally homogeneous cloud extending across the entire domain. The total water mixing ratio and liquid ice static energy are vertically uniform within the initial cloud, where the value of liquid ice static energy is taken from the background sounding at the cloud midpoint in the vertical. Thus, ice water path (IWP) and ice water content are functions of the initial cloud depth and appear consistent with the findings of Feofilov et al. (2015). Here we calculate IWP and ice water content with only cloud ice. The initial cloud's midpoint is at 12.5 km above the surface corresponding with the observed maximum in cloud fraction in the tropics (Hartmann & Berry, 2017; McFarlane et al., 2007; Protat et al., 2010). Convective initiation is aided by prescribed random perturbations in potential temperature of order 0.01 K at every grid point in the cloud layer. All simulations are run until the LW and SW fluxes at the top of the atmosphere become roughly constant with time and the IWP of the cloud drops below 1.0 g/m<sup>2</sup>. Model statistics are computed every 30 simulated seconds. Output is saved every 10 min.

Many sets of simulations are performed to test the sensitivity of the basic conclusions to parameter settings and initialization. To test fundamental physical processes we perform *control* and a *no cloud radiation* (NCR) simulations. In the NCR simulations the model does not feel the radiative perturbations associated with the presence of the cloud or snow. To test the sensitivity to the initial cloud depth, initial cloud depths are varied from 1 to 6 km in 1-km intervals, as shown in Figure 3. For the M2005 and P3 microphysics schemes in the control simulations, thin ice clouds persist for a long time in the upper troposphere.

The effects of simulated clouds on the radiation budget are measured with the SWCRE, LWCRE, and NCRE, computed instantaneously and integrated over time. We calculate the LWCRE and SWCRE as

$$\text{LWCRE} = \text{LWTOA}_{\text{clr}} - \text{LWTOA}, \quad (1)$$

$$\text{SWCRE} = \text{SWTOA}_{\text{clr}} - \text{SWTOA}, \quad (2)$$

where SWTOA and LWTOA are the upward SW and LW radiative fluxes at the top of the atmosphere and *clr* indicates clear sky values. The NCRE is just the LWCRE and SWCRE added together. Integrating the LWCRE, SWCRE, and NCRE over a cloud's lifetime quantifies the full effect that a given initial cloud has on the radiation budget over its life cycle from initialization to disappearance.

## 3. Results

### 3.1. Control Simulation

Because we believe it is the most relevant case, we focus on the deepest initial cloud (6 km). This choice is the most relevant if we consider that all anvil clouds start out as a thick layer of detainment between the top of the convective layer and the freezing level. Our Control simulations show that, for all cloud depths, the IWP and cloud ice mixing ratio rapidly decrease at the beginning as the microphysics and radiative conditions adjust. The nature of this adjustment depends on the initial ice concentration and particle size. Figure 4 shows a strong radiative dipole, with cooling at cloud top and heating at cloud base, which destabilizes the entire layer and drives convection throughout the cloud. The latent heating is significant during the early part of the simulation, but after the initial snow adjustment, radiative heating dominates latent heating in the cloud. A large snow event occurs around 0.1 day in response to the initial convective overturning and rapid conversion of ice to snow, yielding a temporary double dipole in radiative heating. As the snow falls and extends the cloud bottom downward, heating from below becomes more disperse and convection weakens. At around 0.3 days, the snow fallout has greatly thinned, and heating at the elevated cloud bottom becomes strong

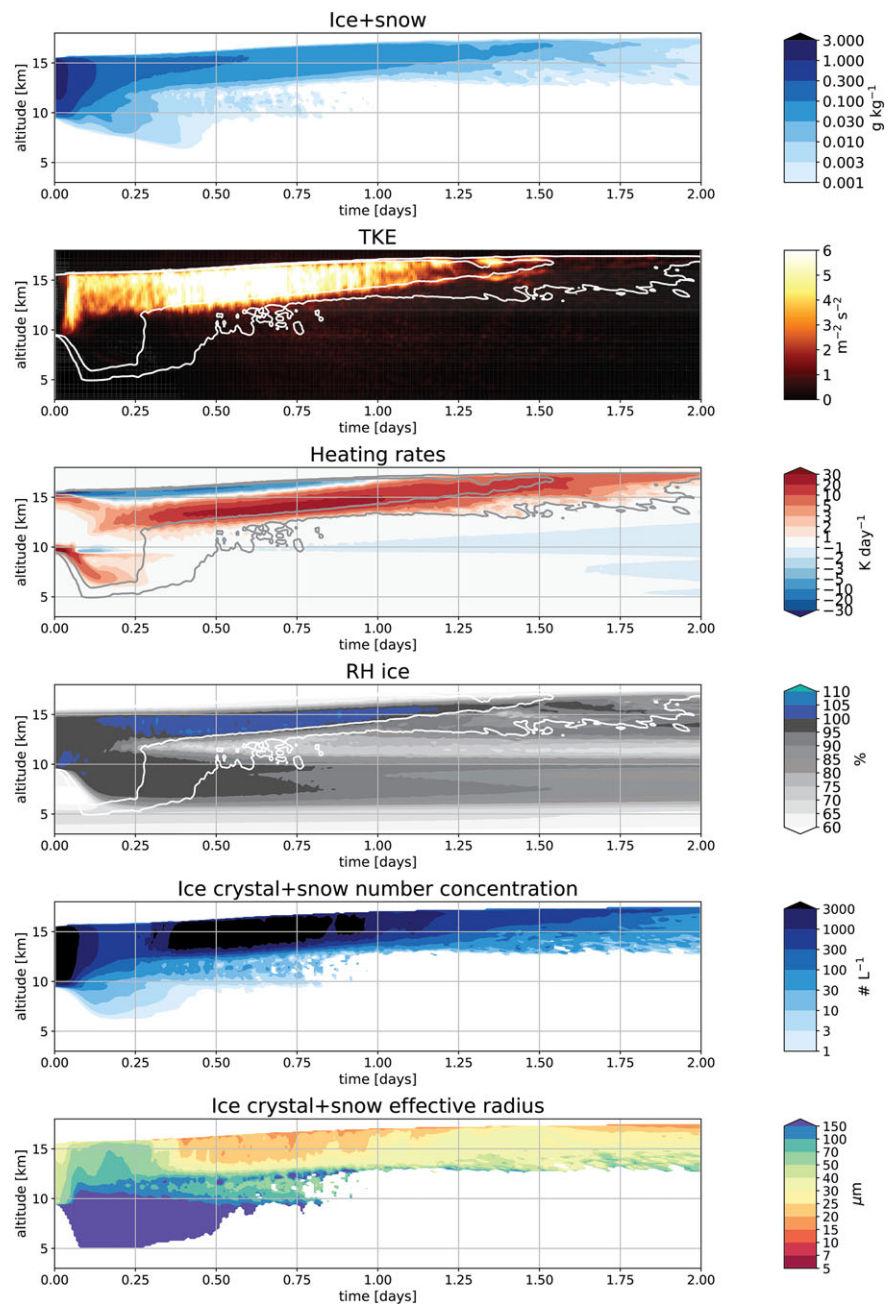


**Figure 4.** (top) Horizontal mean distribution of cloud ice (QI) plus snow (QS) mixing ratios with time for the control case with interactive cloud radiation. (second panel) TKE with time. The white lines are the 0.03- and 0.003-g/kg contours of QI + QS. (third panel) Radiative heating rate with time where red indicates heating and blue indicates cooling. The gray contours are the same QI + QS contours as in the second panel. (fourth panel) Relative humidity with respect to ice. The white contours are the same as above. The transition from unsaturated to supersaturated near cloud bottom corresponds to the transition in sublimation to deposition dominated regions, respectively. (fifth panel) Ice crystal plus snow number concentration. (sixth panel) Ice crystal plus snow effective radius. TKE = turbulent kinetic energy; RH = relative humidity.

enough to reinvigorate convection within the anvil cloud as seen in the turbulent kinetic energy (TKE) field in the second panel of Figure 4. Even when the radiative heating is everywhere positive, TKE is generated because the heating is larger below cloud top. Rising and thinning of the cloud continues through the end of the simulation, though markedly less hydrometer fallout is observed. All clouds, save the 1-km-deep cloud, rise to hit the tropopause at approximately 17-km altitude, becoming thin tropopause cirrus.

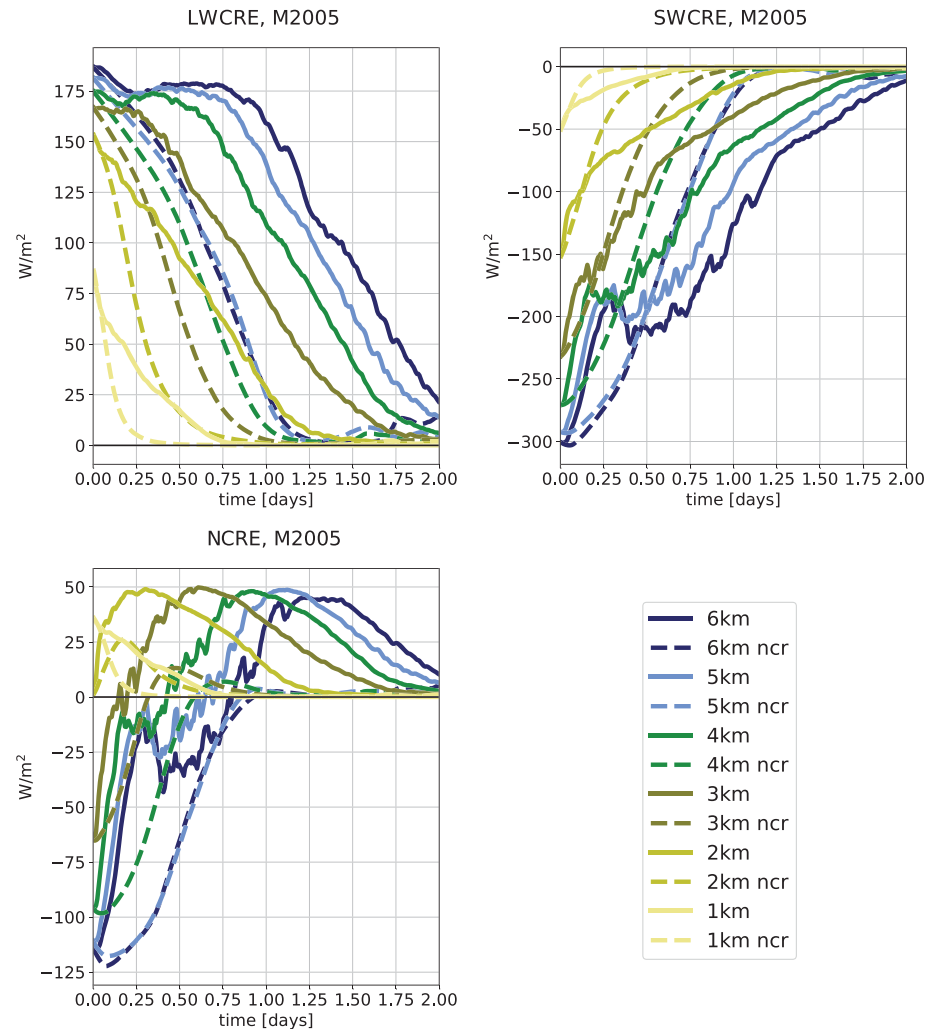


**Figure 5.** LWCRE, SWCRE, and NCRE with time for all cloud depths in the control case (solid) and no cloud radiation case (dashed). Cloud depths progress from light being the thinnest to dark being the thickest. Panels show LWCRE, SWCRE, and NCRE. LWCRE = longwave cloud radiative effect; SWCRE = shortwave cloud radiative effect; NCRE = net cloud radiative effect.

The changing ice content and rising of the cloud play major roles in setting the SWCRE and LWCRE, respectively. The NCRE is shown as a function of time for each anvil cloud depth in Figure 5. Clouds of 1- to 2-km thickness have an initially small positive or negative NCRE compared to the other cloud depths due to their low starting IWP. For 3-km-thick clouds and deeper, the NCRE is initially more notably negative and approaches saturation for clouds more than about 5-km depth. Anvil clouds transition to a positive NCRE at a time dictated by (1) how fast and high the cloud rises, (2) the amount and strength of convection within the cloud, and (3) how quickly the IWP decreases in response. The effect of convection is evident in the NCRE time series through the initial rapid increase at the beginning from the loss of ice mass to snow and the prolonged period of near-neutral NCRE during convective reinvigoration. After the NCRE becomes positive, clouds of different initial thicknesses follow a similar evolution through positive NCRE until dissipation, indicating that the initially thinner clouds can be thought of as a latter stage in an initially thicker cloud's life cycle.

Since we hypothesize that the life cycle of the extended anvil cloud is important in determining net radiative neutrality, we integrate NCRE over time (Figure 6). The integrated NCRE becomes less positive and closer to neutral as the initial cloud depth increases, making the 6-km-deep cloud nearly radiatively neutral over its lifetime. As shown by Hartmann and Berry (2017), Hartmann et al. (2001), and Figure 1, the net radiative neutrality results from a diverse population of clouds spanning a wide range of OLR and albedo values, with thin, high clouds making an important positive contribution to NCRE. Anvil clouds emerging from tropical

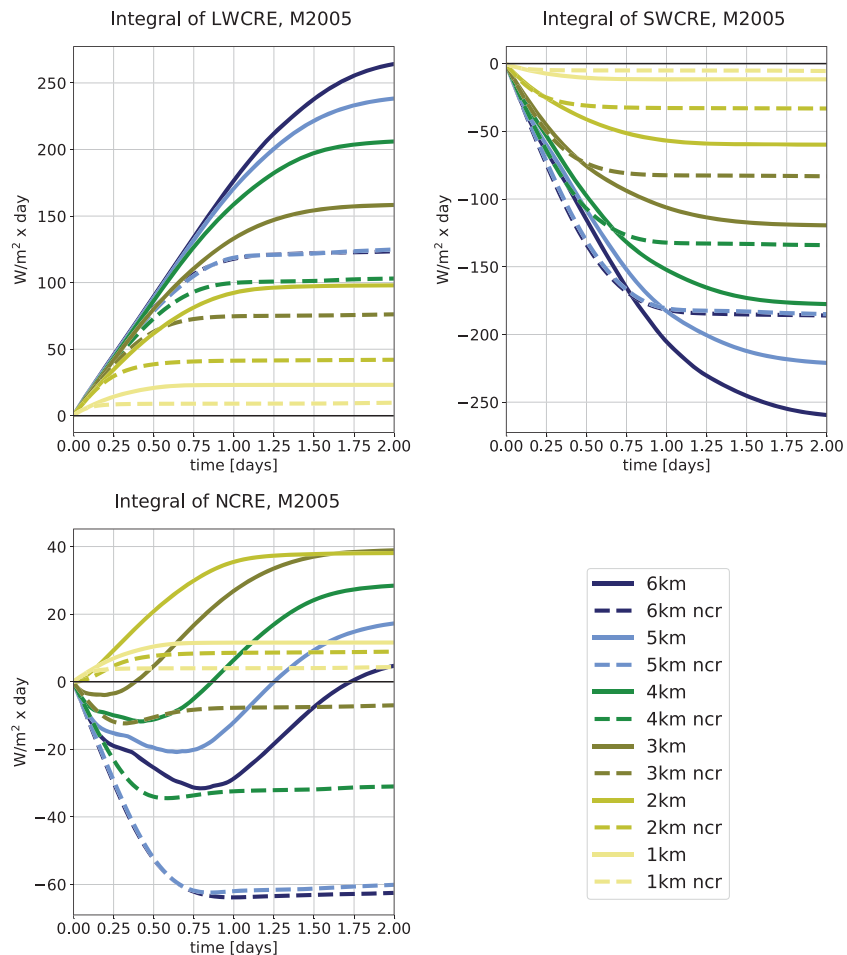


**Figure 6.** Same as Figure 5 but integrated in time. LWCRE = longwave cloud radiative effect; SWCRE = shortwave cloud radiative effect; NCRE = net cloud radiative effect.

convection experience much of this range over their lifetime. Our 6-km-deep cloud simulation is a reasonable representation of the life history of anvil clouds, within the constraints of the simplified model setup used here.

### 3.2. No Interactive Cloud Radiation

In the NCR simulations (Figure 7), the anomalies in radiative heating associated with the presence of the cloud are not felt by the simulation. In this case, instead of rising, the cloud layer slowly sediments and sublimates away in the absence of radiative destabilization. The lack of radiative destabilization and the associated convection within the anvil are also apparent in the total column TKE, which is orders of magnitude smaller in the NCR case than in control case with cloud radiative heating. Consequently, the integrated NCRE in the NCR case is largely negative (Figure 6) due to (1) the cloud remaining optically thicker for longer (increasing the SWCRE) and (2) a lack of lofted thin cirrus (decreasing the LWCRE). In addition, the cloud tends to dissipate sooner without interactive radiation, as seen in the termination of the 0.03 g/kg cloud ice contour at 0.7 days in the NCR case in Figure 7 compared to 1.5 days in the case with interactive radiation. To understand why the cloud radiative interaction makes such a difference, we now look at the microphysical terms in the ice budget.

### 3.3. Total Column Tendencies

The total column mass tendencies of ice plus snow are shown in Figure 8. All processes are substantially different between the control and NCR cases. In the control case, rapid layer overturning due to substantial initial cooling at cloud top and heating at cloud bottom results in rapid thinning of the initial cloud by sedimentation and sublimation. Sublimation, deposition, and sedimentation are the largest tendencies by an order of magnitude for both cases. Sublimation and deposition mostly offset one another within the deep overturning anvil cloud. In the case with cloud-radiative interactions, new particle nucleation commences after the initial

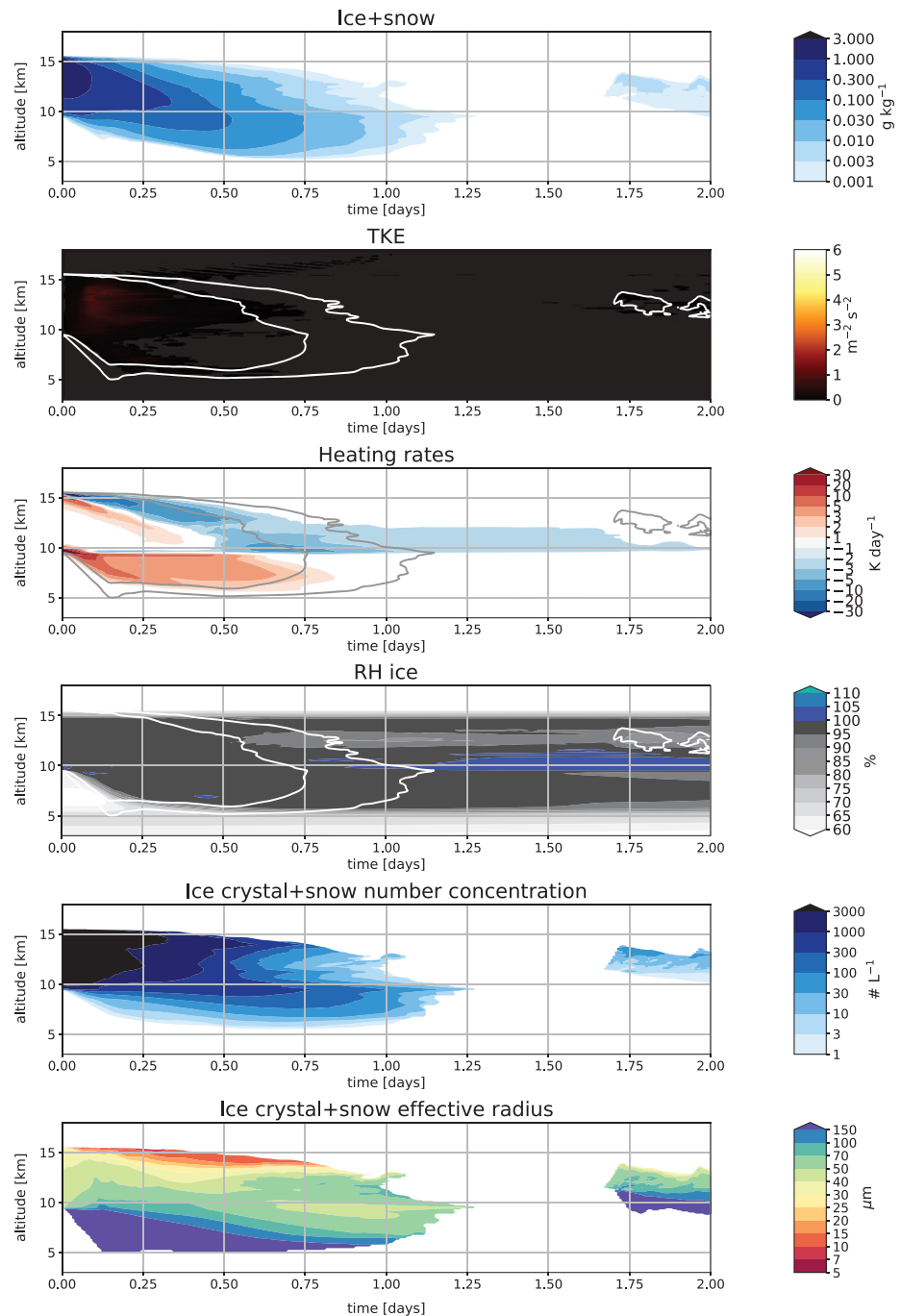


**Figure 7.** Same as Figure 4 but for the no cloud radiation case. The radiative heating in the second panel is the radiative heating that would be observed if the cloud was interacting with the radiation fields. TKE = turbulent kinetic energy; RH = relative humidity.

heavy snow event. Without radiative interactions, the initial rapid overturning does not occur, all the cloud ice tendency terms are smaller, and the cloud retains its large ice mass longer. From the total column tendency, it is apparent that the delayed and reduced loss of ice particles in the case without interactive cloud radiation occurs because the initial rapid overturning does not occur. In the absence of overturning motions, ice crystals are size sorted by gravitational settling, which limits their aggregation efficiency and snow production. This also means that less ice is converted to snow by accretion. Thus, clouds without interactive radiation remain optically thicker for longer.

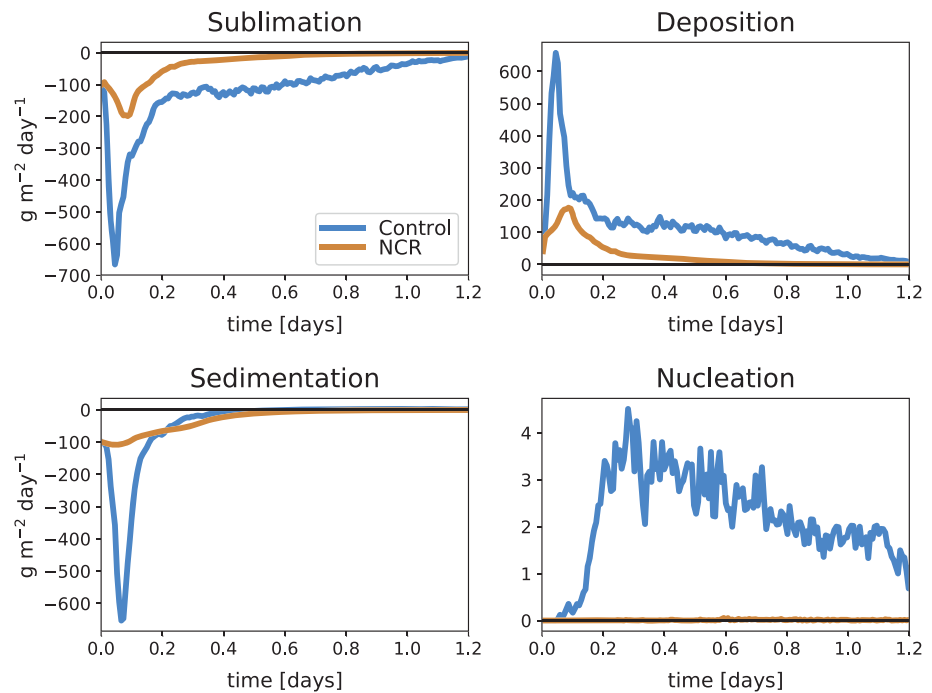


**Figure 8.** Column total microphysical mass tendencies of ice plus snow as a function of time for the control (blue) and NCR (orange) simulations. NCR = no cloud radiation.

### 3.4. Lofting of Thin Cirrus

Vertical profiles of the microphysical tendency terms reveal further information about the role of radiation in producing a thinner but longer-lasting extended anvil cloud. Figure 9 shows the vertical structure of ice tendencies averaged over 0.5 to 0.75 days, when the reinvigoration of convection is strongest. Sublimation and deposition are large and opposite but slightly offset in the vertical. In the control case, this offset dominates layers below 15-km altitude and creates a tripole in the total vertical tendency. The node around 13 km corresponds to the transition from subsaturated to supersaturated with respect to ice (Figure 4). Above 16 km, sedimentation is dominant. Nucleation occurs near the bottom of the ice layer.

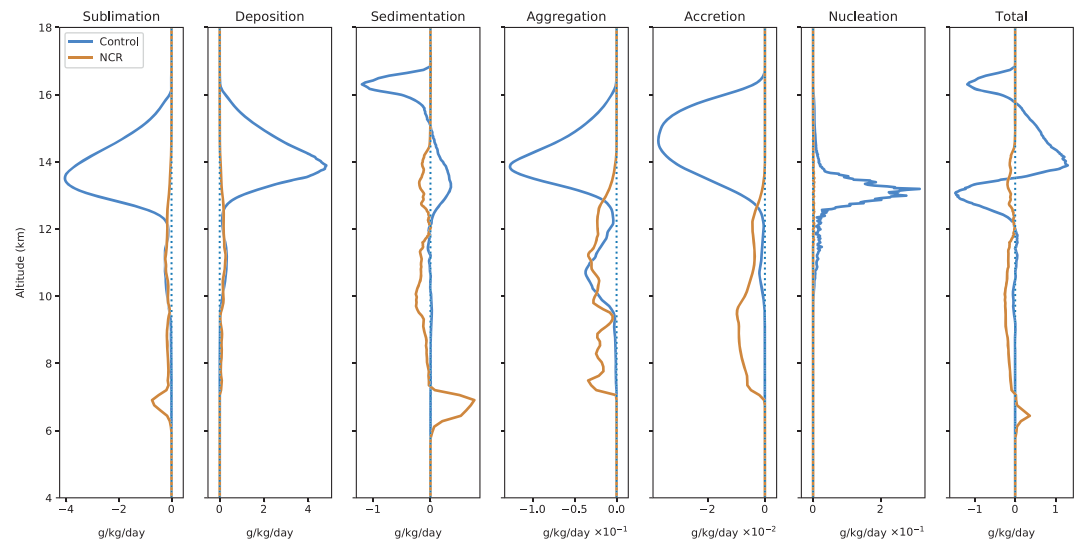


**Figure 9.** Vertical profiles of microphysical tendency terms averaged over 0.5-0.75 days for the 6km cloud. The Control case is shown in blue and the NCR case is shown in orange. The zero line is displayed as a dotted black line on each subplot. Scales on the x-axis for Aggregation, Accretion, and Nucleation are scaled by orders of magnitude for visibility. NCR = no cloud radiation.

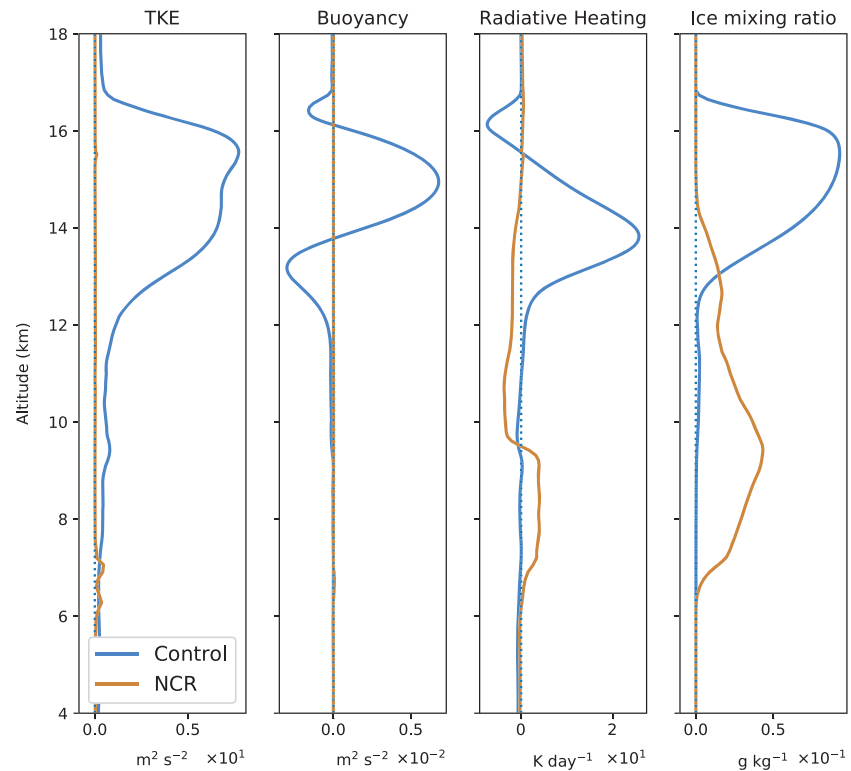


**Figure 10.** Similar to Figure 9, but for convective parameters and ice mixing ratio. Buoyancy and ice mixing ratio have scaled x axes. NCR = no cloud radiation.

Without interactive radiation (NCR case), the cloud is much lower at 0.5–0.75 days after initiation. Sublimation and deposition are much smaller, aligned vertically, and nearly equal. Accretion increases and autoconversion decreases compared to the case with cloud interactions, and no nucleation occurs. Sedimentation dominates the total tendency throughout the cloud layer. Sublimation is larger than deposition below 10 km and has a secondary maximum at 6.5 km where sedimentation delivers excess ice.

The vertical distribution of TKE, buoyancy, radiative heating, and ice mixing ratio averaged over days 0.5–0.75 are shown in Figure 10. Without interactive radiation, little buoyancy and TKE are generated. Thus, without radiatively driven instability, cloud ice is not lofted and sustained and can only sediment, leading to the lower cloud altitude compared to the control. In the control case, cooling at cloud top corresponds to a negative buoyancy signature. Heating from below makes the majority of the cloud layer positively buoyant. A larger minimum in buoyancy is located at the bottom of the cloud at around 13-km altitude, which results from heavy particle loading in this region.

Relative humidity cross sections (Figures 4 and 7) reveal important differences between the control and NCR cases. With radiative interactions, significant supersaturations occur near cloud top in the convective layer that is driven by radiative heating. Observations confirm that such high supersaturations can occur in the upper troposphere (Comstock et al., 2004). In our simulations, the cloud remains saturated with respect to ice through the layer except near cloud bottom where a transition to subsaturation occurs and sublimation becomes dominant over deposition. In the NCR case, since there is no convection, the layer of high supersaturation does not occur. The cloud layer remains at or below saturation.

### 3.5. Microphysical Cycling

Combining the vertical tendencies in Figures 9 and 10, a cycling of parcels through the cloud depth becomes apparent for the control case. At cloud top, parcels are forced downward due to radiative cooling at cloud top, but since the environment is supersaturated with respect to ice, the cloud ice within the parcel sediments along with the descending air. As the parcel continues to descend and adiabatically warm, sublimation exceeds deposition. In the descending branch of the cycle, ice is primarily sublimating but not efficiently due to the ice supersaturation down to approximately 13-km altitude. Across the threshold of saturation, the

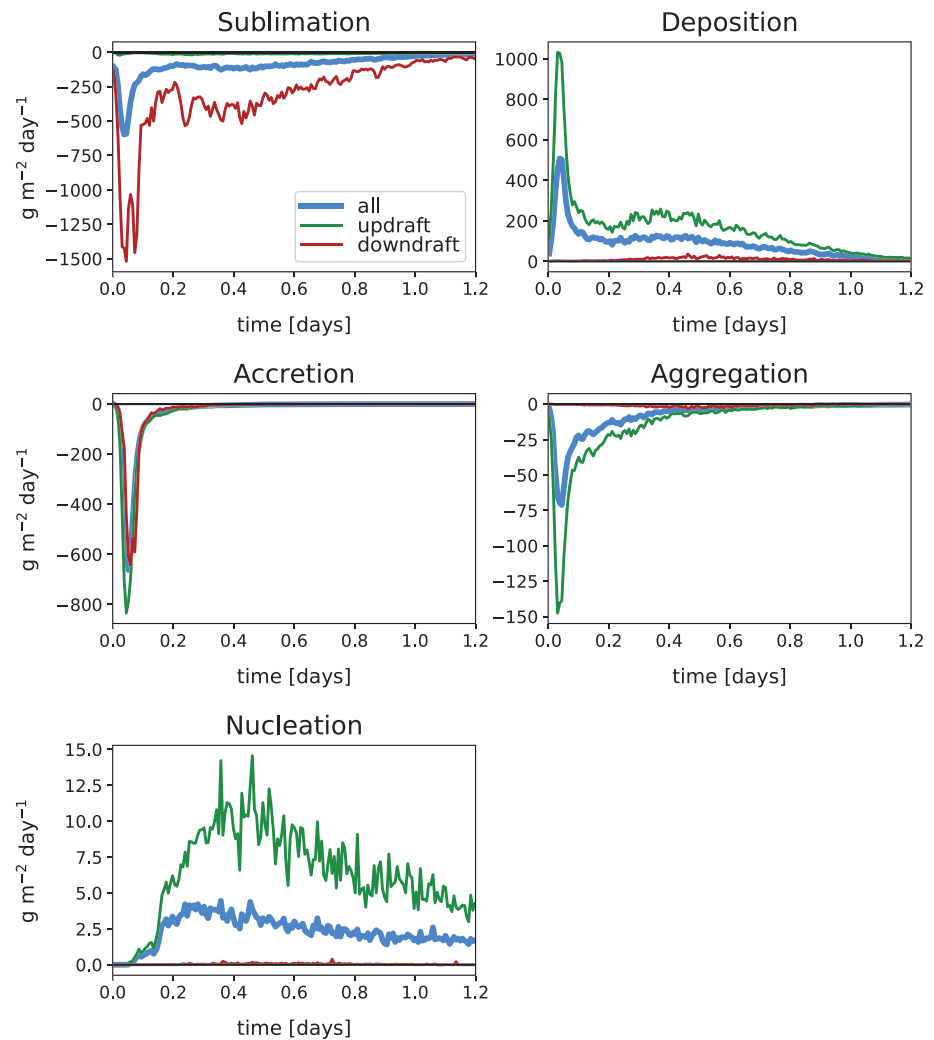


**Figure 11.** Similar to Figure 8, but microphysical mass tendencies for cloud ice are averaged separately for upward and downward moving air.

transition from deposition to sublimation occurs. Radiative heating from below heats the cloud bottom aiding sublimation. Thus, in the horizontal mean, deposition dominates above 13 km, while sublimation dominates below 13 km. As the parcel descends toward cloud bottom, adiabatic warming and radiative heating create a positive buoyancy anomaly, forcing the parcel back upward. Nucleation of new particles occurs and ice mass increases by deposition during the upward trajectory of the parcel. When the parcel reaches the top of the cloud, the cycle begins again.

To illustrate these processes more clearly, microphysical terms are shown separately for upward and downward moving parcels in Figure 11. As one would expect, the sublimation occurs primarily in the downdrafts, and nucleation, deposition, and aggregation occur in the updrafts. This recycling between water vapor and ice within the cloud layer due to the interactions among turbulent, microphysical, and radiative effects helps to sustain the cloud and slow the transition into the regime where cirrus thins and eventually disappears. The water recycling helps to explain how observed cirrus clouds can persist longer than the lifetime of cirrus ice particles (Luo & Rossow, 2004). The positive NCRE in the extended thinning anvil phase offsets the negative NCRE from the thicker anvil earlier in its life cycle so that NCRE neutrality is achieved in the case with cloud radiative effects included.

Nucleation of new ice particles is critical to the maintenance of the anvil cloud in these simulations. To test this we ran a case where nucleation of new particles from vapor was suppressed. In this case the anvil cloud barely survives the snowing phase of the experiment and the elevated ice cloud is gone before 12 hr of simulation.

**Table 1**  
*Simulations Constructed to Test the Sensitivity of the Results to Various Model and Cloud Parameters*

Simulation	Altered parameter
50% Initial QI	Initial ice content 1/2 control value at each level
P3 micro	Uses P3 microphysics scheme (Morrison & Milbrandt, 2015)
Thompson micro	Uses Thompson microphysics scheme (Thompson et al., 2007)
No nucleation	Nucleation of new ice particles is suppressed, M2005
Half water vapor	TOGA COARE water vapor profile halved at all levels
No LSF	No applied large-scale forcing
Double horiz res	$\Delta x = 125$ m
Half vert res	$\Delta z = 50$ m
Large domain	Horizontal domain size = 128 km
13-km Top	Top of initial cloud is at 13 km, same initial ice content as M2005 control

*Note.* Parameters altered with respect to the control simulation are detailed in the right-hand column. TOGA COARE = Tropical Ocean Global Atmosphere Coupled Ocean-Atmosphere Response Experiment; LSF = Large Scale Forcing.

This is true for both the M2005 and P3 microphysics, with the P3 microphysics showing an even quicker demise with no elevated ice cloud surviving the initial snowing phase (not shown). The potential importance of nucleation in anvil clouds is supported by the work of Jensen et al. (2009), who hypothesize that high concentrations of small ice particles sometimes seen in aged anvil cloud may be associated with nucleation associated with waves or turbulence.

Our simulations confirm that the radiative destabilization within an extended upper level ice cloud is fundamentally important to its maintenance and internal microphysical processes. The natural evolution of an initially thick anvil cloud to a thin cirrus cloud can yield a net neutral cloud radiative effect over the life cycle of the anvil cloud. The novel idea here is that the net neutrality of convective clouds in the tropical western Pacific is in large measure a fundamental property that arises from the natural life cycle of anvil clouds. The specific way in which this life cycle evolves is very sensitive to the interaction between radiation, turbulence, and microphysics. The radiative heating and resulting convection within the anvil induce a recycling of ice through a cycle of sublimation and deposition, which is of principal importance. These processes do not guarantee the degree of radiative neutrality observed, which may require additional feedback processes such as that proposed by Hartmann et al. (2001).

#### 4. Sensitivity Studies

Since the processes within anvil clouds described above involve strong interactions between microphysics and dynamics, we conduct a series of experiments to see how our mechanism performs under various

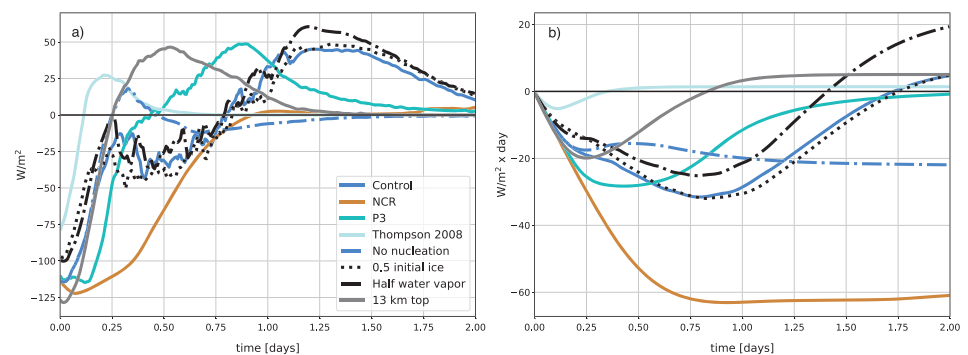


**Figure 12.** NCRE (a) and integrated NCRE (b) of the 6 km deep cloud for several cases. Control is in blue and NCR is in orange. Specifics for the other cases are outlined in Table 1. Negative NCRE values during the No LSF case after 2.0 days is due to the formation of midlevel clouds. NCR = no cloud radiation; NCRE = net cloud radiative effect; LSF = Large Scale Forcing.

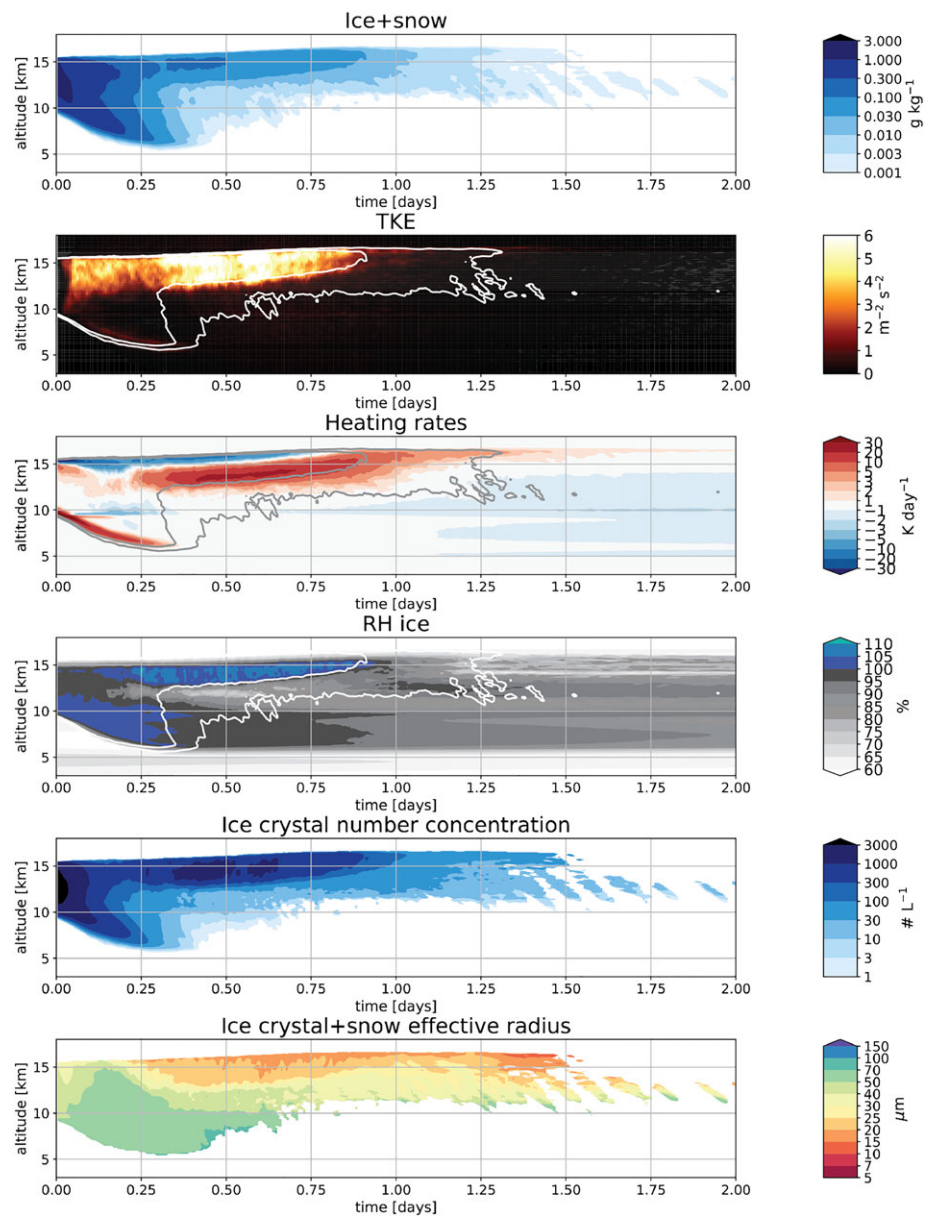


**Figure 13.** Same as Figure 4 but for predicted particle properties microphysics control case. TKE = turbulent kinetic energy; RH = relative humidity.

atmospheric conditions and model configurations. We vary the initial ice content, microphysics scheme, background moisture profile, applied large-scale forcing, horizontal/vertical resolution, and domain size. The parameters of these simulations are detailed in Table 1. Changing the domain resolution, changing the domain size, and turning off the applied large-scale forcing do not affect our basic conclusions.

The ice content of anvil clouds can vary significantly from storm to storm and in different regions. Thus, we conduct another set of simulations where we initialize our anvil cloud with half the amount of cloud ice in grams per kilogram than in the control case. If the initial ice mass is reduced by half (50% initial QI case in Figure 12), less snow production occurs, as expected, but the cloud still rises and thin cirrus is lofted. The lack of snowfall leads to stronger convection, both initially and during reinvigoration, since the radiative heating of the elevated ice cloud is weaker when snow or ice extends lower in the atmosphere (Hartmann & Berry, 2017). Additionally, the reinvigoration phase begins sooner by about a tenth of a day and does not persist as long. The ending structure is similar between the control and 50% initial QI cases.

To understand how the environmental moisture profile can alter anvil cirrus radiation and development, a set of simulations named *half water vapor* is performed. Here the relative humidity of the background sounding is multiplied at all levels by 0.5, shown by the dashed line in Figure 2. Although this profile is not derived from observations of a specific region, we hope it will give insight into the role of upper tropospheric relative humidity in determining cloud structure and NCRE.

The reduction in water vapor in the half water vapor simulations leads to an increase in the integrated NCRE for all simulations (Figure 12). We expect an increase in LWCRE if the cloud remains unchanged, since the clear-sky OLR will increase. It is interesting that the magnitude of both the SWCRE and LWCRE increase. Since less water vapor is below the cloud, the emission temperature felt by the cloud base is higher, which increases the heating at cloud base. This leads to higher TKE values and cloud top heights, increasing the LWCRE. Stronger in-cloud convection enhances the microphysical cycling, which acts to sustain higher IWP values than the control over most of the anvil's lifetime. A larger IWP acts to increase cloud albedo and optical depth. The increase in the clear-sky OLR and cloud top height combine to make the LWCRE increase more than the SWCRE and produce a more positive integrated NCRE, despite the increased cloud albedo.

Since microphysical processes are fundamental to our present arguments, we expect our results are sensitive to the microphysical parameterization. The Thompson microphysics (Thompson et al., 2007) was developed in order to improve upon the accuracy of existing bulk microphysics schemes' quantitative precipitation forecasts, forecasts of water aloft and at the surface, and representations of snow. However, this leads to an increased production of snow, and in our model framework the anvil cloud cannot be sustained as long as for the M2005 microphysics. Feng et al. (2018) compared the Thompson and M2005 schemes in high-resolution simulations of warm season convection over North America. They found that both schemes produced reasonable agreement with observations but that Thompson did a better job of simulating upper level clouds and matching the observed amount of stratiform precipitation. This may indicate the different sensitivities to microphysics scheme in strongly dynamically forced situations, compared to the nearly quiescent ice cloud of our model setup.

With the Thompson microphysics, the cloud life cycle appears to be accelerated, dissipating quickly while still going through the thick and cooling to thin and heating phases (Figure 12). The tendency toward greater snow production in Thompson and greater ice production in M2005 was previously noted in Powell et al. (2012). Even with the abundance of snow creation, the 6-km cloud is still radiatively neutral, although the cloud is short lived.

The P3 scheme produces a life cycle in these experiments that is closer to M2005 than to Thompson. The ice does not last as long and is not lofted as high as for M2005, but all the basic characteristics of the life cycle are similar in the M2005 and P3 microphysics cases (Figure 13). The same period of weak turbulence while the snow falls from below occurs, followed by a period of TKE resurgence when the lower part of the elevated ice cloud is exposed to LW radiation from below. A similar dry layer occurs beneath the ice cloud, and the anvil cloud has small particles at the top and larger particles below. Much of the difference may be attributed to the smaller number concentration in the P3 case, to which a number concentration limiter has been applied. In the P3 case shown here the ice concentration has been limited to  $10^6 \text{kg}^{-1}$ , which is approximately  $2-5 \text{cm}^{-3}$  in the upper troposphere.

For all three microphysics schemes, the cloud goes through a cycle from negative to positive NCRE that tends to produce a neutral integrated effect, even though the magnitude of the cloud effects and the lifetime of the cloud are very different. Further investigation into how to accurately represent small-scale dynamical and microphysical processes in anvil clouds is certainly warranted.

The system modeled here is very idealized and neglects three fundamental processes that could alter anvil cloud life cycles. Allowing for two- or three-dimensional effects of localized anvil clouds could induce mesoscale circulations that balance the radiative heating such as in Dinh et al. (2010), but tests have shown that three-dimensionality and a localized initial cloud show results similar to our two-dimensional uniform cloud initial condition. Synoptic and mesoscale dynamical forcing could drive the clouds sufficiently hard that the in-cloud turbulence is less important than in our quiescent horizontally uniform initial state simulations. In our simulations we simply placed a cloud in a quiescent atmosphere, but in nature extended elevated ice clouds are fed by deep convective cells. This supply of ice may overwhelm the in-cloud turbulent and microphysical processes highlighted here. Single-column model simulations in Hartmann and Berry (2017) showed

less sensitivity to radiative driving when the large-scale forcing was pulsed rather than continuous. In future work we hope to investigate anvil dynamics in the presence of active convection in three dimensions.

## 5. Discussion and Conclusion

We have investigated the role of radiation, in-cloud turbulence, and cloud microphysics in establishing the net neutral cloud radiative effect of tropical anvil clouds by using idealized model simulations. The natural life cycle of thick anvil clouds progressing toward thin cirrus plays a major role in setting the net neutrality by passing through a wide range of OLR and albedo pairings. We could consider the population of clouds observed at any time to be a combination of many convective systems in various stages of their life cycle, or we could consider that even at its mature stage a single mesoscale convective system contains within it a population of clouds with both positive and negative net cloud radiative effects.

In evaluating models, emphasis should be placed on comparing the proportion of thin to thick anvil clouds with observations and understanding how this proportion might be sensitive to surface temperature. Energetic requirements coupled with Clausius-Clapeyron suggest that convective mass flux will decline in a warmed world (Held & Soden, 2006; Pendergrass & Hartmann, 2014). This may result in a decrease in deep convective cloud cover, but if the net radiative effect of the convective clouds remains neutral, it could have little effect on climate sensitivity, contrary to numerous speculations that a reduction in convective cloud area would constitute a strong negative feedback (e.g., Lindzen et al., 2001; Mauritsen & Stevens, 2015). Understanding the physics behind the net radiative neutrality of tropical convective cloud complexes is a prerequisite for reducing the uncertainty associated with their climate feedbacks.

We have shown by comparing our control case to one without interactive cloud radiation that radiative destabilization drives the radiative properties of anvil clouds by initially thinning thick anvils then lofting and maintaining thin cirrus. Without radiation the cloud simply sediments and sublimates away in contrast to the lofting seen in the control case. Radiation drives convection within the anvil that leads to greater persistence of the anvil cloud by recycling ice through vapor within the cloud layer. Lofting of clouds results from the convergence of vertical ice transport near cloud top supported by radiative heating near cloud base, which also rises due to heating and sedimentation. Profiles of cloud ice mixing ratio become increasingly top heavy with time. The maintenance of anvil clouds is tied to a cycling between cloud ice and water vapor through sublimation and deposition as parcels of air are circulated through the cloud layer. Sublimation and deposition, the two largest microphysical tendencies throughout the simulations, are almost equal and opposite, but deposition is stronger in the top half of the cloud and sublimation is stronger near cloud base. Nucleation of new ice particles is critical to the maintenance of the elevated ice cloud in these simulations.

Our findings support the idea that better understanding of the net radiative neutrality of tropical convective clouds requires more careful analysis of the roles of radiative heating, cloud microphysics, and turbulent mixing within extended anvil clouds. Such deeper understanding would enable more confident predictions about how the ratio of rainy cores to extended upper level ice clouds might change in a warmed climate. Will these proportions remain fixed in a warmed Earth, so that the net radiative effect of tropical clouds remains neutral, or will the ratio of thick to thin anvils change to give a potentially important cloud feedback on climate change? Will representing the physics correctly require including the interactions of turbulence and microphysics within the extended anvil cloud? Can the relevant processes be adequately parameterized so that computationally efficient global climate models can accurately represent the key processes?

### Acknowledgments

This work derives for the Masters Thesis of Sara E. Berry. We would like to thank Guangxing Lin and Jiwen Fan for sharing their implementation of the WRF P3 microphysics in SAM. We acknowledge support from DOE through Grant DE-SC0012580 (S. E. B. and D. L. H.), from the Pacific Northwest National Laboratory through its E3SM project under task order 400723 (B. G.), from the National Science Foundation through grant AGS-1549579 (P. N. B.), and the Swiss National Science Foundation grant P2EZP2-178485 (B. G.). The data shown in Figure 1 are available from Atmospheric Sciences Data Center at NASA Langley Research Center. The model used is publicly available at <http://rossby.msrc.sunysb.edu/marat/SAM.html>. Our thanks to the developers of this model.

### References

- Ackerman, T. P., Liou, K. N., Valero, F. P. J., & Pfister, L. (1988). Heating rates in tropical anvils. *Journal of Atmospheric Science*, *45*(10), 1606–1623.
- Berry, E., & Mace, G. G. (2014). Cloud properties and radiative effects of the asian summer monsoon derived from A-Train data. *Journal of Geophysical Research: Atmospheres*, *119*, 9492–9508. <https://doi.org/10.1002/2014JD021458>
- Boehm, M. T., Verlinde, J., & Ackerman, T. P. (1999). On the maintenance of high tropical cirrus. *Journal of Geophysical Research*, *104*(D20), 24,423–24,433. <https://doi.org/10.1029/1999JD900798>
- Chen, J. P., McFarquhar, G. M., Heymsfield, A. J., & Ramanathan, V. (1997). A modeling and observational study of the detailed microphysical structure of tropical cirrus anvils. *Journal of Geophysical Research*, *102*(D6), 6637–6653. <https://doi.org/10.1029/96JD03513>
- Churchill, D. D., & Houze, R. A. (1991). Effects of radiation and turbulence on the diabatic heating and water budget of the stratiform region of a tropical cloud cluster. *Journal of Atmospheric Science*, *48*(7), 903–922. [https://doi.org/10.1175/1520-0469\(1991\)048<0903:Eorato>2.0.Co;2](https://doi.org/10.1175/1520-0469(1991)048<0903:Eorato>2.0.Co;2)
- Comstock, J. M., Ackerman, T. P., & Turner, D. D. (2004). Evidence of high ice supersaturation in cirrus clouds using ARM Raman lidar measurements. *Geophysical Research Letters*, *31*, L11106. <https://doi.org/10.1029/2004GL019705>

- Deng, M., Mace, G. G., & Wang, Z. (2016). Anvil productivities of tropical deep convective clusters and their regional differences. *Journal of Atmospheric Science*, 73(9), 3467–3487. <https://doi.org/10.1175/jas-d-15-0239.1>
- Dinh, T. P., Durran, D. R., & Ackerman, T. P. (2010). Maintenance of tropical tropopause layer cirrus. *Journal of Geophysical Research*, 115, D02104. <https://doi.org/10.1029/2009JD012735>
- Dobbie, S., & Jonas, P. (2001). Radiative influences on the structure and lifetime of cirrus clouds. *Quarterly Journal of the Royal Meteorological Society*, 127(578), 2663–2682. <https://doi.org/10.1256/smsqj.57807>
- Fan, J. W., Comstock, J. M., & Ovchinnikov, M. (2010). The cloud condensation nuclei and ice nuclei effects on tropical anvil characteristics and water vapor of the tropical tropopause layer. *Environmental Research Letters*, 5(4), 44005.
- Feng, Z., Leung, L. R., Houze, R. A., Hagos, S., Hardin, J., Yang, Q., et al. (2018). Structure and evolution of mesoscale convective systems: Sensitivity to cloud microphysics in convection-permitting simulations over the united states. *Journal of Advances in Modeling Earth Systems*, 10, 1470–1494. <https://doi.org/10.1029/2018MS001305>
- Feofilov, A. G., Stubenrauch, C. J., & Delanoë, J. (2015). Ice water content vertical profiles of high-level clouds: Classification and impact on radiative fluxes. *Atmospheric Chemistry and Physics*, 15, 12,327–12,344. <https://doi.org/10.5194/acp-15-12327-2015>
- Field, P. R., Hogan, R. J., Brown, P. R. A., Illingworth, A. J., Choulaton, T. W., & Cotton, R. J. (2005). Parametrization of ice-particle size distributions for mid-latitude stratiform cloud. *Quarterly Journal of the Royal Meteorological Society*, 131(609), 1997–2017. <https://doi.org/10.1256/qj.04.134>
- Fu, Q. (1996). An accurate parameterization of the solar radiative properties of cirrus clouds for climate models. *Journal of Climate*, 9(9), 2058–2082.
- Fu, Q., Krueger, S. K., & Liou, K. N. (1995). Interactions of radiation and convection in simulated tropical cloud clusters. *Journal of Atmospheric Science*, 52(9), 1310–1328. [https://doi.org/10.1175/1520-0469\(1995\)052<1310:IORACI>2.0.CO;2](https://doi.org/10.1175/1520-0469(1995)052<1310:IORACI>2.0.CO;2)
- Gettelman, A., Liu, X., Ghan, S. J., Morrison, H., Park, S., Conley, A. J., et al. (2010). Global simulations of ice nucleation and ice supersaturation with an improved cloud scheme in the community atmosphere model. *Journal of Geophysical Research*, 115, D18216. <https://doi.org/10.1029/2009JD013797>
- Gu, Y., & Liou, K. N. (2000). Interactions of radiation, microphysics, and turbulence in the evolution of cirrus clouds. *Journal of Atmospheric Science*, 57(15), 2463–2479. [https://doi.org/10.1175/1520-0469\(2000\)057<2463:IFORMAT>2.0.CO;2](https://doi.org/10.1175/1520-0469(2000)057<2463:IFORMAT>2.0.CO;2)
- Harrison, E. F., Minnis, P., Barkstrom, B. R., Ramanathan, V., Cess, R. D., & Gibson, G. G. (1990). Seasonal variation of cloud radiative forcing derived from the Earth radiation budget experiment. *Journal of Geophysical Research*, 95(D11), 18,687–18,703. <https://doi.org/10.1029/JD095iD11p18687>
- Harrop, B. E., & Hartmann, D. L. (2016). The role of cloud radiative heating within the atmosphere on the high cloud amount and top-of-atmosphere cloud radiative effect. *Journal of Advances in Modeling Earth Systems*, 8, 1391–1410. <https://doi.org/10.1002/2016ms000670>
- Hartmann, D. L., & Berry, S. E. (2017). The balanced radiative effect of tropical anvil clouds. *Journal of Geophysical Research: Atmospheres*, 122, 5003–5020. <https://doi.org/10.1002/2017JD026460>
- Hartmann, D. L., & Larson, K. (2002). An important constraint on tropical cloud-climate feedback. *Geophysical Research Letters*, 29(20), 1951. <https://doi.org/10.1029/2002GL015835>
- Hartmann, D. L., Moy, L. A., & Fu, Q. (2001). Tropical convection and the energy balance at the top of the atmosphere. *Journal of Climate*, 14(24), 4495–4511. [https://doi.org/10.1175/1520-0442\(2001\)014<4495:TCATEB>2.0.CO;2](https://doi.org/10.1175/1520-0442(2001)014<4495:TCATEB>2.0.CO;2)
- Hartmann, D. L., Ockert-Bell, M. E., & Michelsen, M. L. (1992). The effect of cloud type on earth's energy balance: Global analysis. *Journal of Climate*, 5(11), 1281–1304. [https://doi.org/10.1175/1520-0442\(1992\)005<1281:teocto>2.0.co;2](https://doi.org/10.1175/1520-0442(1992)005<1281:teocto>2.0.co;2)
- Hartmann, D. L., & Short, D. A. (1980). On the use of earth radiation budget statistics for studies of clouds and climate. *Journal of Atmospheric Science*, 37(6), 1233–1250. [https://doi.org/10.1175/1520-0469\(1980\)037<1233:OTUOER>2.0.CO;2](https://doi.org/10.1175/1520-0469(1980)037<1233:OTUOER>2.0.CO;2)
- Held, I. M., & Soden, B. J. (2006). Robust responses of the hydrological cycle to global warming. *Journal of Climate*, 19(21), 5686–5699.
- Heysmsfield, A. J., & Miloshevich, L. M. (2003). Parameterizations for the cross-sectional area and extinction of cirrus and stratiform ice cloud particles. *Journal of Atmospheric Science*, 60(7), 936–956. [https://doi.org/10.1175/1520-0469\(2003\)060<0936:Pftcsa>2.0.Co;2](https://doi.org/10.1175/1520-0469(2003)060<0936:Pftcsa>2.0.Co;2)
- Houze, R. (1982). Cloud clusters and large-scale vertical motions in the tropics. *Journal of the Meteorological Society of Japan*, 60, 396–410.
- Jensen, E. J., Lawson, P., Baker, B., Pilsen, B., Mo, Q., Heysmsfield, A. J., et al. (2009). On the importance of small ice crystals in tropical anvil cirrus. *Atmospheric Chemistry and Physics*, 9(15), 5519–5537. <https://doi.org/10.5194/acp-9-5519-2009>
- Jensen, E. J., Pfister, L., & Toon, O. B. (2011). Impact of radiative heating, wind shear, temperature variability, and microphysical processes on the structure and evolution of thin cirrus in the tropical tropopause layer. *Journal of Geophysical Research*, 116, D12209. <https://doi.org/10.1029/2010JD015417>
- Jensen, E. J., Ueyama, R., Pfister, L., Bui, T. V., Alexander, M. J., Podglajen, A., et al. (2016). High-frequency gravity waves and homogeneous ice nucleation in tropical tropopause layer cirrus. *Geophysical Research Letters*, 43, 6629–6635. <https://doi.org/10.1002/2016gl069426>
- Jensen, E. J., Ueyama, R., Pfister, L., Bui, T. V., Lawson, R. P., Woods, S., et al. (2016). On the susceptibility of cold tropical cirrus to ice nuclei abundance. *Journal of Atmospheric Science*, 73(6), 2445–2464. <https://doi.org/10.1175/jas-d-15-0274.1>
- Khairoutdinov, M. F., & Randall, D. A. (2003). Cloud resolving modeling of the ARM summer 1997 IOP: Model formulation, results, uncertainties, and sensitivities. *Journal of Atmospheric Science*, 60, 607–625. [https://doi.org/10.1175/1520-0469\(2003\)060<0607:CRMOTA>2.0.CO;2](https://doi.org/10.1175/1520-0469(2003)060<0607:CRMOTA>2.0.CO;2)
- Korolev, A. V., Emery, E. F., Strapp, J. W., Cober, S. G., & Isaac, G. A. (2013). Quantification of the effects of shattering on airborne ice particle measurements. *Journal of Atmospheric and Oceanic Technology*, 30(11), 2527–2553. <https://doi.org/10.1175/jtech-d-13-00115.1>
- Lindzen, R. S., Chou, M. D., & Hou, A. Y. (2001). Does the earth have an adaptive infrared iris? *Bulletin of the American Meteorological Society*, 82(3), 417–432.
- Liou, K. (1986). Influence of cirrus clouds on weather and climate processes: A global perspective. *Monthly Weather Review*, 114, 1167–1199. [https://doi.org/10.1175/1520-0493\(1986\)114<1167:IOCCOW>2.0.CO;2](https://doi.org/10.1175/1520-0493(1986)114<1167:IOCCOW>2.0.CO;2)
- Lopez, M. A., Hartmann, D. L., Blossey, P. N., Wood, R., Bretherton, C. S., & Kubar, T. L. (2009). A test of the simulation of tropical convective cloudiness by a cloud-resolving model. *Journal of Climate*, 22(11), 2834–2849. <https://doi.org/10.1175/2008JCLI2272.1>
- Luo, Z., & Rossow, W. B. (2004). Characterizing tropical cirrus life cycle, evolution, and interaction with upper-tropospheric water vapor using lagrangian trajectory analysis of satellite observations. *Journal of Climate*, 17(23), 4541–4563. <https://doi.org/10.1175/3222.1>
- Mapes, B. E., & Houze, R. A. (1993). Cloud clusters and superclusters over the oceanic warm pool. *Monthly Weather Review*, 121(5), 1398–1415. [https://doi.org/10.1175/1520-0493\(1993\)121<1398:ccasot>2.0.co;2](https://doi.org/10.1175/1520-0493(1993)121<1398:ccasot>2.0.co;2)
- Mauritsen, T., & Stevens, B. (2015). Missing iris effect as a possible cause of muted hydrological change and high climate sensitivity in models. *Nature Geoscience*, 8(5), 346–351. <https://doi.org/10.1038/ngeo2414>
- McFarlane, S. A., Mather, J. H., & Ackerman, T. P. (2007). Analysis of tropical radiative heating profiles: A comparison of models and observations. *Journal of Geophysical Research*, 112, D14218. <https://doi.org/10.1029/2006JD008290>

- Mitchell, D. L., Rasch, P., Ivanova, D., McFarquhar, G., & Nousiainen, T. (2008). Impact of small ice crystal assumptions on ice sedimentation rates in cirrus clouds and GCM simulations. *Geophysical Research Letters*, *35*, L09806. <https://doi.org/10.1029/2008GL033552>
- Mlawer, E. J., Taubman, S. J., Brown, P. D., Iacono, M. J., & Clough, S. A. (1997). Radiative transfer for inhomogeneous atmospheres: RRTM, a validated correlated-k model for the longwave. *Journal of Geophysical Research*, *102*, 16,663–16,682. <https://doi.org/10.1029/97JD00237>
- Morrison, H., Curry, J. A., & Khvorostyanov, V. I. (2005). A new double-moment microphysics parameterization for application in cloud and climate models. Part I: Description. *Journal of Atmospheric Science*, *62*(6), 1665–1677.
- Morrison, H., & Milbrandt, J. A. (2015). Parameterization of cloud microphysics based on the prediction of bulk ice particle properties. Part I: Scheme description and idealized tests. *Journal of Atmospheric Science*, *72*(1), 287–311. <https://doi.org/10.1175/jas-d-14-0065.1>
- Pendergrass, A. G., & Hartmann, D. L. (2014). The atmospheric energy constraint on global-mean precipitation change. *Journal of Climate*, *27*(2), 757–768. <https://doi.org/10.1175/jcli-d-13-00163.1>
- Powell, S., Houze, R. A., Kumar, A., & McFarlane, S. A. (2012). Comparison of simulated and observed continental tropical anvil clouds and their radiative heating profiles. *Journal of Atmospheric Science*, *69*, 2662–26,817. <https://doi.org/10.1175/JAS-D-11-0251.1>
- Protat, A., Delanoe, J., Plana-Fattori, A., May, P. T., & O'Connor, E. J. (2010). The statistical properties of tropical ice clouds generated by the West African and Australian monsoons, from ground-based radar-lidar observations. *Quarterly Journal of the Royal Meteorological Society*, *136*, 345–363.
- Protopapadaki, S. E., Stubenrauch, C. J., & Feofilov, A. G. (2017). Upper tropospheric cloud systems derived from IR sounders: Properties of cirrus anvils in the tropics. *Atmospheric Chemistry and Physics*, *17*, 3845–3859. <https://doi.org/10.5194/acp-17-3845-2017>
- Ramanathan, V., Cess, R. D., Harrison, E. F., Minnis, P., Barkstrom, B. R., Ahmad, E., & Hartmann, D. (1989). Cloud-radiative forcing and climate: Results from the Earth Radiation Budget Experiment. *Science*, *243*, 57–63.
- Sanderson, B. M., Piani, C., Ingram, W. J., Stone, D. A., & Allen, M. R. (2008). Towards constraining climate sensitivity by linear analysis of feedback patterns in thousands of perturbed-physics gcm simulations. *Climate Dynamics*, *30*(2-3), 175–190. <https://doi.org/10.1007/s00382-007-0280-7>
- Sherwood, S. C. (1999). On moistening of the tropical troposphere by cirrus clouds. *Journal of Geophysical Research*, *104*(D10), 11,949–11,960.
- Thompson, G., Field, P. R., Rasmussen, R. M., & Hall, W. D. (2007). Explicit forecasts of winter precipitation using an improved bulk microphysics scheme. Part II: Implementation of a new snow parameterization. *Monthly Weather Review*, *136*, 5095–5115. <https://doi.org/10.1175/2008MWR2387.1>
- Wall, C. J., & Hartmann, D. L. (2018). Balanced cloud radiative effects across a range of dynamical conditions over the tropical West Pacific. *Geophysical Research Letters*, *45*, 11,490–11,498. <https://doi.org/10.1029/2018GL080046>
- Wall, C. J., Hartmann, D., Thieman, M., Smith, W. J., & Minnis, P. (2018). The lifecycle of anvil clouds and the top-of-atmosphere radiation balance over the tropical West Pacific. *Journal of Climate*. <https://doi.org/10.1175/JCLI-D-18-0154.1>
- Wielicki, B., Barkstrom, B., Harrison, E., Lee, R. I., Smith, G., & Cooper, J. (1996). Clouds and the Earth's Radiant Energy System (CERES): An Earth observing system experiment. *Bulletin of the American Meteorological Society*, *77*(5), 853–868.
- Zender, C. S., & Kiehl, J. T. (1994). Radiative sensitivities of tropical anvils to small ice crystals. *Journal of Geophysical Research*, *99*(D12), 5,869–25,880.